Tidal stream energy resource assessment of the Anglesey Skerries

Tidal Stream Energy Resource Assessment of the Anglesey Skerries

Sena Serhadlıoğlu, Thomas A.A. Adcock, Guy T. Houlsby, Scott Draper, Alistair G.L. Borthwick

PII: S2214-1669(13)00040-4
DOI: http://dx.doi.org/10.1016/j.ijome.2013.11.014
Reference: IJOME 26

To appear in:

Please cite this article as: S. Serhadlıoğlu, T.A.A. Adcock, G.T. Houlsby, S. Draper, A.G.L. Borthwick, Tidal Stream Energy Resource Assessment of the Anglesey Skerries, (2013), doi: http://dx.doi.org/10.1016/j.ijome.2013.11.014

Tidal Stream Energy Resource Assessment of the Anglesey Skerries

Sena Serhadlıoğlu[#1], Thomas A.A. Adcock[#2], Guy T. Houlsby[#3], Scott Draper[*4], Alistair G.L. Borthwick[+5]

[#]*Department of Engineering Science, University of Oxford*
Parks Road Oxford OX1 3PJ UK
[1]sena.serhadlioglu@eng.ox.ac.uk
[2]thomas.adcock@eng.ox.ac.uk
[3]guy.houlsby@eng.ox.ac.uk

[*]*Centre for Offshore Foundation Systems, University of Western Australia*
Crawley WA 6009, Australia
[4]scott.draper@uwa.edu.au

[+]*School of Engineering, University of Edinburgh*
Mayfield Road Edinburgh EH9 3JL UK
[5]alistair.borthwick@ed.ac.uk

***Abstract*— Many candidate sites for tidal stream power devices can be classified as headlands. This paper analyses one such site, off Anglesey. In order to investigate the disturbance to the local flow field due to the operation of tidal arrays and evaluate the extractable power at the site, a two-dimensional depth-averaged shallow water model of the naturally occurring tidal dynamics of the south-west UK and Irish Sea has been developed and validated. In the model, the effect of tidal arrays is represented by line discontinuities where upstream and downstream heads are related by Linear Momentum Actuator Disk Theory. A parametric study to investigate the importance of array locations, the connectivity of the arrays and local blockage effects on the available power has been undertaken. General conclusions from this analysis are that it is generally advantageous to arrange tidal turbines in long rows rather than as a number of rows in series, and that arrays with higher local blockage outperform arrays with lower blockage.**

***Keywords*— Anglesey, tidal hydrodynamics, shallow water model, available power, turbine efficiency.**

I. Introduction

Tidal power obtained from turbines offers potentially large renewable power supply to the UK [1]. Draper [2] considered various idealised coastline geometries, which can induce fast tidal flows and so are of interest in placing tidal turbines. One such geometry is a headland.

Various approaches have been taken to assess the resource of headland sites. The first is based on the undisturbed kinetic energy flux [1]. This approach provides an incorrect estimate of the resource, as there is no direct proportionality between the kinetic energy flux and available power [3]. A second, numerical modelling, approach has been applied by Blunden and Bahaj [4] to resource assessment offshore of the Portland Bill headland, in which the far-field effects of the tidal array deployment are represented by means of an additional bed roughness coefficient in the governing equations. A third approach, Draper *et al.* [3] analyse an idealised headland in which the turbine arrays are described using a near-field approximation that is embedded in a two-dimensional shallow water solver. The near-field approach enables a distinction to be made between the available power and the total power extracted from the site. Assuming that the tidal devices are evenly spaced and the length of the downstream mixing zone is sufficiently smaller than the mesh discretisation, Draper [2] demonstrate that the effects of tidal arrays can be represented using a line sink of momentum. This approach is used in the present paper. The method has also been applied to the Pentland Firth by Adcock *et al.* [5] and has been compared to laboratory measurements of flow around a headland in [6].

This work considers the methodology presented in [3] and applies it to analyse the available power in the Anglesey Skerries region. A brief summary of the model specifications and validation of the model are presented in Section II and Section III respectively. The parametric study results are given in Section IV, and the disturbance to the flow field is analysed in Section V.

II. Numerical Model Details

A. Numerical Scheme

In this paper the tidal dynamics is modelled by solving the two-dimensional hyperbolic shallow water equations [7], [8] using a Runge-Kutta discontinuous Galerkin method [9], [10], [11].

The particular hydrodynamic model used here is the discontinuous Galerkin version of ADCIRC [12], which has been modified to account for the head loss across a turbine array by means of a line sink of momentum [2]. The associated momentum sink is computed using Linear Momentum Actuator Disk Theory (LMADT, [13]).

In LMADT analysis, the tidal device is represented as a porous disk placed in a constrained flow control volume, and the mass and momentum conservation laws and Bernoulli equation then applied between different stations. The method leads to an equation relating the change in water surface

elevation upstream and downstream of the turbines after wake mixing. The surface elevation difference depends on the upstream flow conditions and the thrust applied to the flow by the turbines.

As the discontinuous Galerkin method approximates the solution locally at each element, it is then possible to include a discontinuity in the surface elevations through a modification in the numerical flux calculations [2]. The implementation and verification of this procedure within the DG-ADCIRC model has been described in [14].

Using LMADT as a sub-model within the depth-integrated code, it is possible to distinguish between the power available to the turbines and the total power extracted from the stream, which is the sum of the available power and the power dissipated in wake mixing behind the turbines [13]. The results presented in this paper focus on the available power which represents an upper bound for the shaft power that could be produced in real turbines.

B. Model Details

A numerical model has been constructed of the south-west coast of UK including the Irish Sea. In a previous study of the tidal dynamics of the model area, Howarth [15] found the Irish Sea to be a small system that does not respond directly to the geophysical forces. Thus the naturally occurring currents in the Irish Sea are driven by the interaction between two tidal waves: one entering the Atlantic Ocean entering through St. George's Channel, the other entering through the Malin Shelf Sea and the North Channel.

The model has three open boundaries, each of which is used for tidal forcing. The first boundary, with the Atlantic to the southwest, is set just beyond the continental shelf in order to include the quarter-wave length resonance effect in the Bristol Channel. The second boundary is located at the western end of the English Channel. The third is at the North Channel between Ulster and Galloway. Semi-diurnal M_2 and S_2 tidal constituents are used to force the model at the open boundaries. It is assumed that the water levels at these boundaries are unaffected by the disturbance caused by the presence of tidal turbines in the interior of the domain.

The model mesh includes inter-tidal zones (Figure 1) along the Cumbrian and Lancashire coasts in order to model correctly reflected waves directed towards the eastern Irish Sea. A wetting and drying algorithm is used to model the moving shoreline in the inter-tidal zones, following [16].

The mesh is unstructured except in the region where rows of tidal turbines are to be deployed. Within this area a structured mesh of elements is embedded. The local mesh size varies from 200 m close to the Anglesey Headland to over 1500 m close to the continental shelf. Figure 1 shows a portion of the mesh fitted to the eastern Irish Sea.

A quadratic bed friction term is applied within the model, with the local bed stress components given by

$$\tau_x = \rho C_D u\sqrt{u^2+v^2}\,, \quad \tau_y = \rho C_D v\sqrt{u^2+v^2}\,, \tag{1}$$

where ρ is the density of seawater, C_D is the drag coefficient, u and v are the horizontal depth-averaged tidal current velocity components. In calibrating the model, it was found that the best fit to field observations after harmonic analysis was obtained by setting $C_D = 0.0025$. The model was run for a complete spring-neap cycle, and the results compared against current velocity observations provided by the British Oceanography Data Centre and tidal water levels obtained from Admiralty Charts.

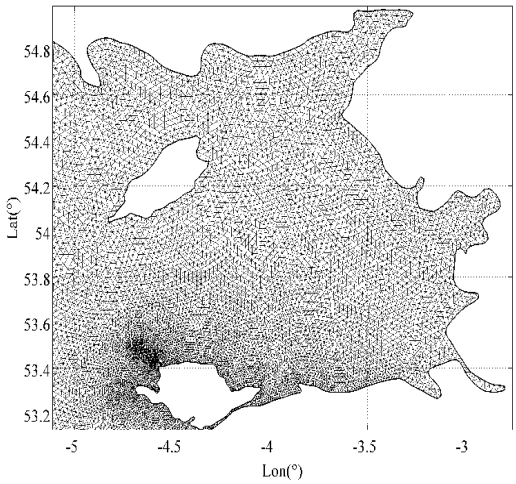

Figure 1 A portion of the two-dimensional unstructured triangular mesh, focusing on the Irish Sea in the region of the Cumbrian and Lancashire coasts.

III. Model Validation

A. Water Levels

In terms of water surface elevation, model validation was undertaken against observed data obtained from the Admiralty Tide Tables for M_2 (Table 1) and S_2 (Table 2) constituents [17]. The model results are in very close agreement with the observations for both amplitude and phase. The water level amplitudes agree to within 5% and the small phase differences suggest that the model predicts the time of high water correct to within eight minutes.

The model results indicate that the tidal range differs significantly between the Irish and Welsh-English coasts. This behaviour is also discussed in [15] where it is suggested that the main reason for this difference is the Coriolis force, which deflects the propagating wave towards the eastern Irish Sea.

Harmonic analysis of the model predictions indicates that degenerate M_2 and S_2 amphidromes are generated off the east coast of Ireland.

Figure 2 shows the predicted M_2 tidal constituent amplitude distribution, locating the amphidromic point (indicated by the dark blue region). It is stated in [18] that this amphidromic system transmits tidal power towards the north of the Irish Sea, where a standing wave forms, enhancing the tidal amplitudes towards the Welsh coasts.

TABLE 1 TIDAL HARMONIC ANALYSIS COMPARISONS FOR M_2 CONSTITUENT

Location	*Coordinates*	*Observations*		*DG-ADCRIRC*	
		$H_n(m)$	$\varphi_n(°)$	$H_n(m)$	$\varphi_n(°)$
Holyhead	53° 19'N 04° 37'W	1.81	292	1.80	292
Cemaes Bay	53° 25'N 04° 27'W	2.13	307	2.12	304
Amlwch	53° 25'N 04° 20'W	2.30	305	2.26	307
Moelfre	53° 20'N 04° 14'W	2.47	308	2.42	311
Trywn Dinmor	53° 19'N 04° 03'W	2.47	310	2.49	312
Beaumaris	53° 16'N 04° 05'W	2.57	312	2.51	313
Port Trecastell	53° 12'N 04° 30'W	1.50	278	1.57	277
Trearddur Bay	53° 16'N 04° 37'W	1.56	280	1.61	280

TABLE 2 TIDAL HARMONIC ANALYSIS COMPARISONS FOR S_2 CONSTITUENT

Location	*Coordinates*	*Observations*		*DG-ADCRIRC*	
		$H_n(m)$	$\varphi_n(°)$	$H_n(m)$	$\varphi_n(°)$
Holyhead	53° 19'N 04° 37'W	0.59	329	0.59	333
Cemaes Bay	53° 25'N 04° 27'W	0.71	345	0.67	345
Amlwch	53° 25'N 04° 20'W	0.75	345	0.71	350
Moelfre	53° 20'N 04° 14'W	0.81	348	0.76	354
Trywn Dinmor	53° 19'N 04° 03'W	0.80	351	0.78	356
Beaumaris	53° 16'N 04° 05'W	0.82	356	0.79	357
Port Trecastell	53° 12'N 04° 30'W	0.50	320	0.53	317
Trearddur Bay	53° 16'N 04° 37'W	0.54	315	0.54	320

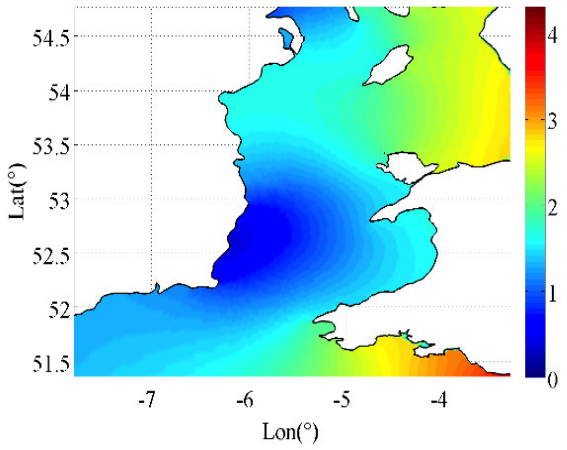

Figure 2 M_2 tidal amplitudes in the Irish Sea obtained from harmonic analysis of the predicted water levels.

B. Currents

Measurements of tidal currents are more susceptible to noise, and tend to be of shorter duration than measurements of water levels [18]. The reliability of the recorded current data is also affected by the elevation of the velocity gauge above the seabed [19]. Data acquired near the seabed are highly sensitive to the exact nature of the local boundary layer, which in turn means that the extrapolation of such data to depth-averaged values is not robust. Current amplitude comparisons are possible using measurements recorded closer to the top of the water column. In this work, the field current data are related to the depth-integrated current in the model using the $1/7^{th}$ power law profile [20], as the actual profile is unknown.

The observed data are obtained from the British Oceanographic Data Centre. The coordinates of the selected gauge is 53°17'N 4°55'W, which is located north-west of Holyhead. The bathymetric depth is 44.0 m, and the readings were conducted 31.0 m above the sea floor.

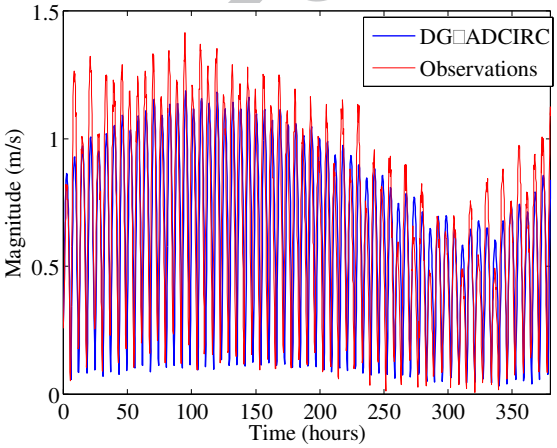

Figure 3 Predicted and observed tidal current magnitude time histories at a gauge north-west of Holyhead. Observed data provided by the British Oceanographic Data Centre.

Figure 3 displays the predicted and observed tidal velocity magnitude time histories;

Figure 4 shows the corresponding tidal current directions with time. During ebb tide the flow velocity is under-predicted, whereas during spring tide it is over-predicted. A possible explanation for this discrepancy might be the bed-friction coefficient applied in the model. The level of agreement shown here indicates that the model is capturing the dominant tidal hydrodynamics. There are several possible causes for the discrepancy, including noise in the field measurements. Furthermore, it is well known that depth-integrated models do not capture all the physics of the flows around a headland [21].

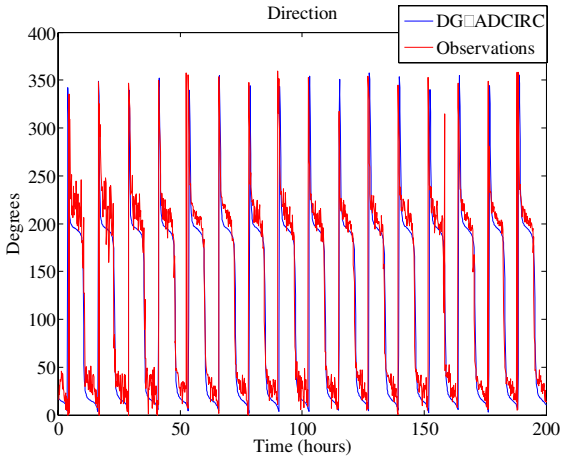

Figure 4 Predicted and observed tidal current direction time histories at a gauge north-west of Holyhead. Observed data provided by the British Oceanographic Data Centre.

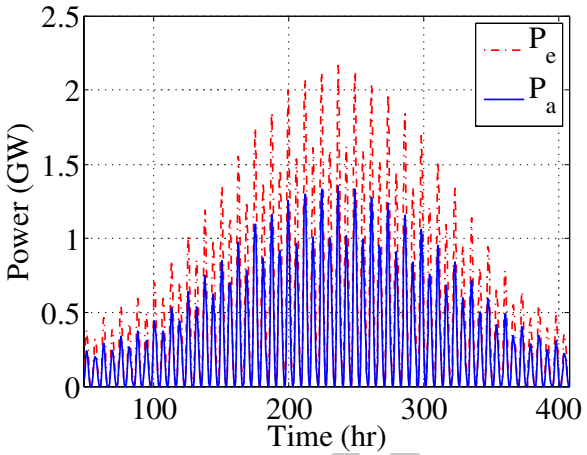

Figure 5 Raw data time series indicating the power extracted from the stream (P_e) and power available to the turbines (P_a) for B = 0.5, α_4 = 0.5, and array configuration ASA1+ASA2

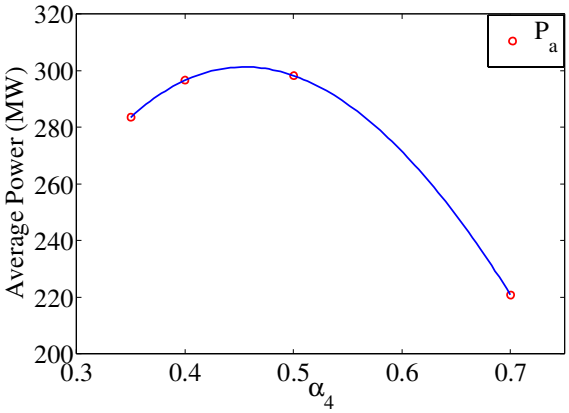

Figure 6 Evaluation of the maximum available power (P_a) with respect to averaged power values obtained for different α_4 for B = 0.5 and array configuration ASA1+ASA2

IV. Power Analysis

This section describes the parametric study for assessing the available power in the vicinity of the Anglesey Skerries.

In the present work, the effect of turbine devices on the local flow field is instead represented by a line sink of momentum, following Draper [3]. A parametric study is undertaken to examine the effects of location and connectivity of the arrays for specified local blockage ratio and wake velocity coefficient, α_4, on the available power.

Using LMADT, for prescribed flow conditions, local blockage ratio (B), and wake velocity coefficient (α_4), it is possible to compute the time series of power available to the turbines and the total power removed from the stream. As explained in [22], there is an optimum wake velocity coefficient that maximises the available power. This value is dependent on the turbine arrangement as well as the coastal features near the area of interest, and the optimum may vary through the spring-neap cycle [5], [23]. However, here we employ a constant wake velocity coefficient throughout the cycle, so that our calculated values will be slightly less than the maximum that would be determined if a variable wake velocity coefficient were to be taken into account. In the present analysis, a range of wake velocity coefficients is considered in order to evaluate the optimum α_4 value from which to compute the maximum available power.

Figure 5 presents the raw power data obtained from a particular test case for a spring-neap cycle. In this case, B = 0.5 and α_4 = 0.5 for the specific array configuration, ASA1+ASA2 (see Figure 7 for the array location).

Averaging the obtained available power over a tidal cycle and repeating the same procedure for each α_4 for a fixed B, it is possible to evaluate the optimum wake velocity coefficient. This is achieved by fitting a spline to the averaged power values (Figure 6). In the rest of this paper, the results are presented for the optimum wake velocity coefficient, α_4 – *i.e.* when the available power is maximised.

A. *Location*

The naturally occurring flow around a headland with realistic bathymetry is highly complex, and so the optimum location to install an array of tidal devices is not obvious. Whilst it may appear reasonable at first sight to use the undisturbed kinetic energy flux to guide the location of turbine array deployments [3], this can be further complicated by the existence of turbines causing flow diversion (see Section V). Figure 7 indicates several trial locations for tidal turbine deployment offshore of the Skerries. The area selected for the analysis is based on two factors. First, the naturally occurring kinetic energy flux is relatively higher than other regions around the Anglesey headland. Second, the bathymetry of the area is favourable for tidal farm deployment.

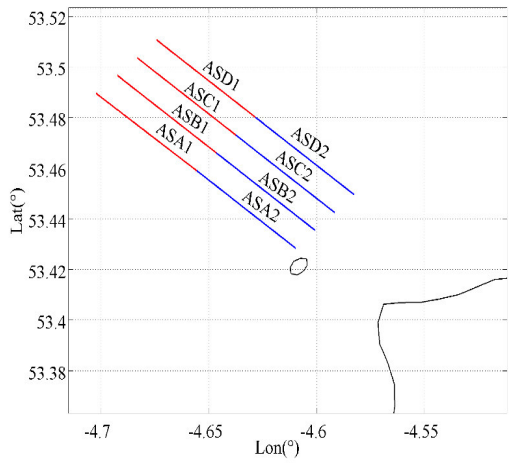

Figure 7 Selected locations of tidal turbine arrays extending towards NE of the Anglesey Skerries

The nomenclature for array configurations is based on the placement of the arrays in the SW-NE direction (ASA being the furthest SW and ASD the furthest NE) and how far the arrays are located away from the Anglesey coastline. Arrays that are further offshore are labelled as Region 1, and those closer to the Skerries as Region 2. Each array has a total length of 4.5 km and is placed approximately 1 km apart from the next array. The arrays are located in regions with varying depths. From Table 3 it can be seen that the mean depths in Region 1 are greater than in Region 2. The arrays in Region 1 hence have a larger swept area of turbines compared to the turbines located in Region 2, when working with a specified local blockage ratio.

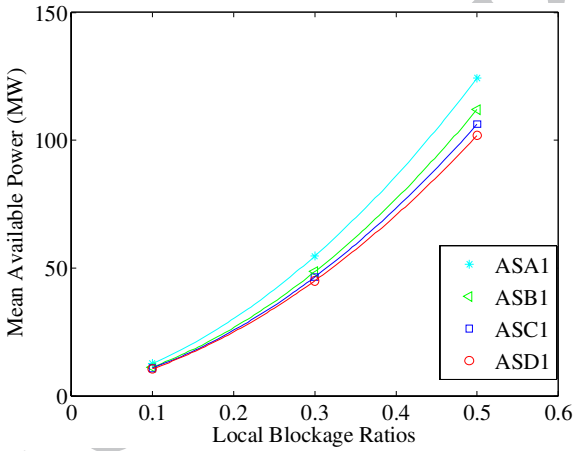

Figure 8 Maximum available power as a function of blockage ratio for the arrays located in Region 1

Table 3 summarises the maximum available power and the total power extracted from the sites and for different blockage ratios, obtained for the optimum wake velocity coefficients.

TABLE 3 POWER VALUES FOR DIFFERENT BLOCKAGE RATIOS AT OPTIMUM WAKE VELOCITY COEFFICIENTS

Location	*Blockage*	*Opt.* α_4	$P_{available}$ *(MW)*	$P_{extracted}$ *(MW)*	*Average Depth (m)*
	0.1	0.35	12.7	20.5	
ASA1	0.3	0.37	54.7	97.7	55.4
	0.5	0.46	124.3	211.3	
	0.1	0.35	11.3	18.1	
ASB1	0.3	0.37	48.6	87.4	57.5
	0.5	0.45	112	192.9	
	0.1	0.35	10.9	17.5	
ASC1	0.3	0.37	46.5	83.1	54.9
	0.5	0.46	106.3	181.5	
	0.1	0.35	10.6	17.1	
ASD1	0.3	0.37	45	80.4	53.3
	0.5	0.46	101.9	172.1	
	0.1	0.35	17.2	27.7	
ASA2	0.3	0.39	70	122	36.3
	0.5	0.50	145.3	230.1	
	0.1	0.35	16.6	26.8	
ASB2	0.3	0.39	67.3	116.6	37.8
	0.5	0.49	139.8	222.8	
	0.1	0.35	13.5	21.8	
ASC2	0.3	0.39	57.1	99.9	43.6
	0.5	0.48	124.5	202.5	
	0.1	0.35	12.1	19.6	
ASD2	0.3	0.38	51.7	91	47.2
	0.5	0.46	116	195.9	

In the table, it is evident that arrays placed closer to the Skerries (Figure 9) extract more power when compared to arrays deployed further offshore (Figure 8).

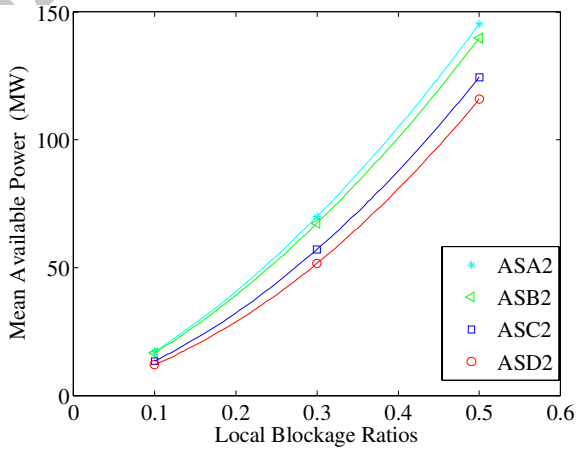

Figure 9 Maximum available power as a function of blockage ratio for the arrays located in Region 2

Despite the fact that the turbines placed in Region 2 have smaller swept areas, they produce considerably more power than the turbines in Region 1. This difference is shown by calculating the power produced per swept area. An example for this can be given by focusing on ASA1 and ASA2 turbine arrays. For a high blockage test case (B = 0.5), the power per swept area for ASA1 array is 0.997 kW/m^2, whereas this value is 1.781 kW/m^2 in ASA2. A similar relationship is observed

for other arrays located in different regions when using fixed blockage ratios.

B. *Array Connectivity*

This section examines the effect of multiple array deployment on array performance. Studies such as by Adcock *et al.* [24] and [25] have shown that there is significant interaction between multiple rows of arrays installed at a given site. Here, we investigate the effect of this interaction on the available power. Following the same methodology for computing the maximum available and extracted power values, Table 4 lists the results obtained from several combinations of array deployments. The table considers the maximum available and extracted power values for parallel (*i.e.* ASA1+ASA2) and series array connections (*i.e.* ASA2+ASB2) respectively. The "gain factor" is defined as the maximum available power with rows of turbines deployed at the same time, relative to the sum of the maximum available power from the rows of turbines deployed on their own.

TABLE 4 MAXIMUM AVAILABLE POWER ESTIMATES FOR SERIAL AND PARALLEL ARRAY CONFIGURATIONS FOR VARIOUS BLOCKAGE RATIOS

Arrays	*Blockage*	*Opt.* α_4	$P_{available}$ (*MW*)	$P_{extracted}$ (*MW*)	*Gain Factor*
ASA1+ASA2	0.1	0.35	30.2	48.7	1.010
	0.3	0.38	130.8	232.5	1.049
	0.5	0.46	301.2	517	1.117
ASB1+ASB2	0.1	0.35	28.1	45.1	1.007
	0.3	0.37	121.8	219.7	1.051
	0.5	0.45	284.5	494.8	1.130
ASC1+ASC2	0.1	0.35	24.6	39.7	1.008
	0.3	0.37	108.4	196.7	1.046
	0.5	0.44	260.3	461.3	1.128
ASD1+ASD2	0.1	0.35	22.9	37	1.009
	0.3	0.36	101.4	185.2	1.049
	0.5	0.44	245.2	434.3	1.125
ASA2+ASB2	0.1	0.35	32.4	52.3	0.959
	0.3	0.44	114.6	183.1	0.835
	0.5	0.58	199.1	280.2	0.698
ASA2+ASC2	0.1	0.35	29.8	48.1	0.971
	0.3	0.42	110.4	181.7	0.869
	0.5	0.56	199.9	289	0.741
ASA2+ASD2	0.1	0.35	28.7	46.2	0.980
	0.3	0.41	109.6	182.4	0.901
	0.5	0.54	205.6	305.7	0.787
ASA2+ASB2+ ASC2+ASD2	0.1	0.36	54.2	86.2	0.912
	0.3	0.48	167.9	253.1	0.682
	0.5	0.64	257	337.6	0.489

Interpreting the results with respect to the array combinations, it is evident that connecting the arrays in parallel is more advantageous. The power available to the turbine in parallel connection is higher than the sum of the two arrays installed in isolation. An example can be given by focusing on the ASA arrays using a high blockage case (B = 0.5). When the individual available power values are summed, the total power is found to be 269.6 MW, whereas Table 4 shows that this is an underestimate of the actual value. For the ASA1+ASA2 configuration, the available power is 301.2 MW. There is approximately 12% power gain above the sum of the two individual array configurations. This percentage gain diminishes with decreasing blockage ratio because less thrust is applied to the flow.

For arrays connected in series, it is found that the available power reduces. Consider the ASA2 and ASB2 arrays in series for B = 0.5. In this case, the sum of individual available power outputs is 285.1 MW whereas the maximum available power is computed to be 199.1 MW. For a highly blocked flow where a large thrust is applied, it is more advantageous to put the arrays in parallel than in series. On the other hand, for a low blockage case, as the disturbance in the flow field is less; the penalty from placing turbines in series is less severe.

In general, arrays interact constructively when connected in parallel and, interact in a destructive manner when deployed in series.

V. HYDRODYNAMIC EFFECTS OF POWER EXTRACTION

One of the main objectives of this study is to evaluate the change in the flow field in the presence of tidal devices. Local to the turbines, there will be a significant change to the flow field with increased flow between turbines that mixes with the slower moving flow, which has based through the rotor plane downstream of the turbines. This complex mixing process cannot be modelled accurately with a depth-integrated model. In the present model, this intra-turbine mixing is accounted for in the sub-grid scale model using linear momentum actuator disk theory (LMADT). Even though, the model does not consider the change to the flow field around a turbine directly, large-scale changes due to the operation of an array of turbines can be estimated.

To investigate the change in velocity flow field, let us consider arrays ASA2, ASB2, ASC2 and ASD2 connected in series for B = 0.5. Figure 10 provides a snapshot of the naturally occurring flood tide in the vicinity of the Anglesey Skerries. The average flow velocity observed in the vicinity of the area is 2.1 m/s. Once the arrays are installed, the flow bypasses the arrays, mainly on the offshore side.

Figure 11 shows a snapshot of the flow field in the presence of tidal arrays deployed. It is evident that the arrays provide additional resistance to the flow. Downstream of the arrays, the velocity magnitude decreases significantly due to the power extraction. Figure 12 plots the difference between the two flow fields. It can be seen that the flow diversion is not symmetric and the bypass flow towards the ocean side is more enhanced than in the Skerries region. The flow diversion indicates that the available power is restricted with respect to the thrust applied to the flow in a partially blocked flow regime.

The flow disturbance is quantified by computing the change in the M_2 tidal harmonic. We consider an array configuration that gives the maximum total power loss: ASA1+ASA2 parallel array for B = 0.5 and α_4 = 0.5. The model is run for an entire spring-neap cycle and comparisons are undertaken against natural flow conditions.

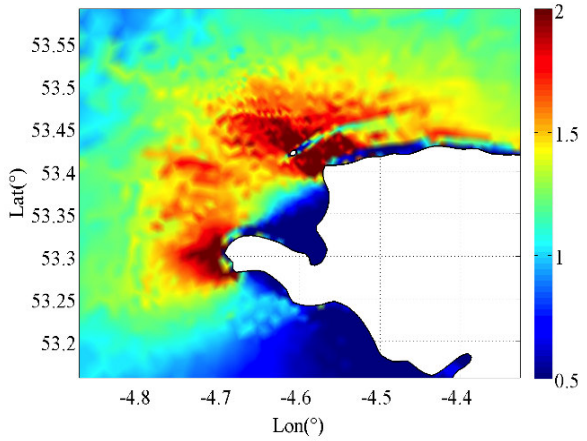

Figure 10 Natural velocity flow field occurring around the Anglesey Skerries. The legend is in meters.

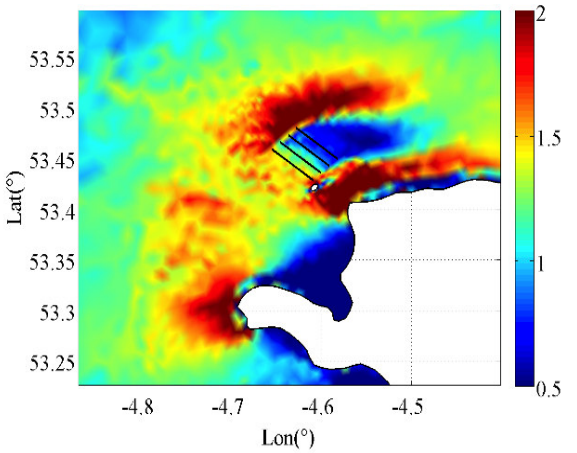

Figure 11 Current velocity plot for a parallel tidal array (ASA2+ASB2+ASC2+ASD2) deployment around the Anglesey Skerries. The legend is in m/s.

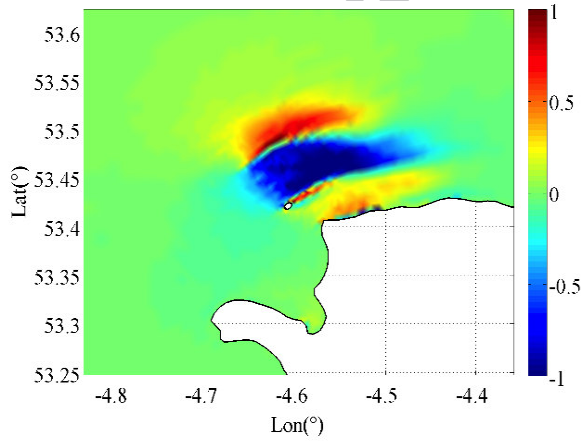

Figure 12 Change in the velocity flow field with respect to the deployment of tidal arrays ASA2+ASB2+ASC2+ASD2 in the vicinity of the Skerries. The existence of the arrays causes flow diversion. The legend is in m/s.

Harmonic analysis of the model results for the ASA1+ASA2 configuration shows that the change in M_2 amplitudes is less than 3%. Arrays placed to the north of the Anglesey headland have a large influence on the tidal amplitudes around Anglesey Island. Table 5 shows the computed values for the M_2 tidal harmonic constituent at several locations around Anglesey and the Irish Sea. It should be noted that the change is insignificant as far as tidal amplitude is concerned. Figure 13 plots the relevant M_2 amplitude change, focusing on the Anglesey Skerries region.

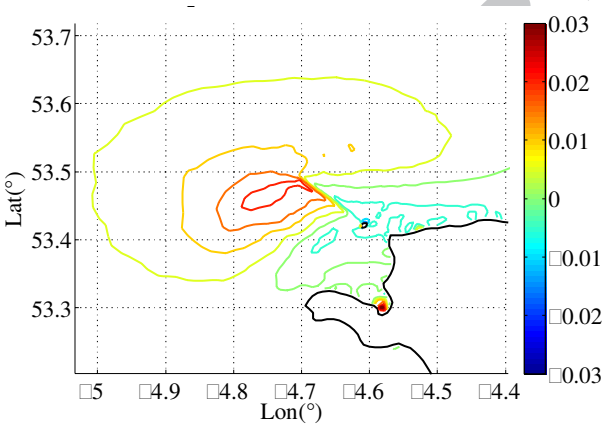

Figure 13 M_2 tidal amplitude changes in the vicinity of the tidal array ASA1+ASA. The legend is in meters.

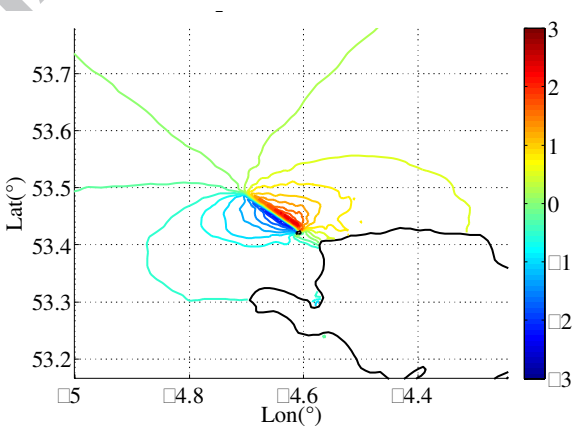

Figure 14 M_2 tidal constituent phase change in the Irish Sea. The legend is in degrees.

Figure 14 plots the phase of the M_2 constituent in the Irish Sea, and the change in the vicinity of the arrays is less than 4 degrees. Upstream of the arrays the phase decreases by 2 degrees, whereas an increment of 2.5 degrees occurs downstream. This implies that high tides are delayed by approximately 5 min immediately before the array location.

TABLE 5 HARMONIC ANALYSIS: M_2 TIDAL CONSTITUENT

Location	*Coordinates*	*Natural Case (model predictions)*		*ASA1+ASA2 for B=0.5*	
		$H_n(m)$	$\varphi_n(°)$	$H_n(m)$	$\varphi_n(°)$
Holyhead	53° 19'N 04° 37'W	1.80	292	1.80	291.4
Amlwch	53° 25'N 04° 20'W	2.26	307	2.25	307.5
Trywn Dinmor	53° 19'N 04° 03'W	2.49	312	2.48	312.4
Port Trecastell	53° 12'N 04° 30'W	1.57	277	1.57	276.6
Port St. Mary	54° 02'N 04° 46'W	1.81	323	1.81	323.1
Aberdaron	52° 47'N 04° 43'W	1.41	252	1.42	251.7

Table 5 summarises the model predictions with respect to the M_2 tidal constituent amplitudes and phases. Even for high blockage, the tidal dynamics within the system does not alter significantly.

VI. CONCLUSIONS

A two-dimensional finite element model of the south-west UK including the Irish Sea has been constructed and validated for simulating the natural tides occurring in the region of the Anglesey Skerries. The numerical model represents turbine arrays by means of a line sink of momentum controlled by upstream flow condition, blockage ratio and wake velocity coefficient. A parametric study has considered the effects of array location, and array configuration in series or in parallel.

The model simulations indicate that more power can be extracted by turbine arrays when placed closer to the Skerries. The bypass flow is found to be greater on the offshore side than regions closer to the Skerries. This result agrees well with the findings of an idealised headland case studied by [9].

As for the connectivity of the arrays, especially for high blockage ratios, it is seen that extending the length of an array further offshore (parallel connectivity) is more effective than placing arrays in series.

To examine the disturbance caused by turbine arrays to the local hydrodynamics, analysis has been undertaken of the change of M_2 water level. It is found that neither the amplitude nor the phase of the M_2 constituent change significantly, even at maximum power extraction. However, more substantial local changes occur to the tidal currents close to the turbine arrays.

ACKNOWLEDGMENTS

This research has been commissioned and funded by the Energy Technologies Institute as part of the PerAWaT project. The calculations were carried out at the Oxford Supercomputing Centre.

Finally, we would like to acknowledge that the bathymetric data and the coastline details were obtained from SeaZONE.

REFERENCES

[1] Black and Veatch Ltd. Phase II: UK tidal stream energy assessment, Technical Report, 2005.

[2] S. Draper (2011) Tidal stream energy extraction in coastal basins, DPhil Thesis, University of Oxford.

[3] S. Draper, A.G.L. Borthwick and G.T. Houlsby (2013) Energy potential of a tidal fence deployed near a coastal headland, *Phil. Trans. Royal Society*, A., **371**:20120176.

[4] L.S. Blunden and A.S. Bahaj (2006) Initial evaluation of tidal stream energy resources at the Portland Bill, UK, *Renew. Energy*, **31**, pp: 121-132.

[5] T.A.A. Adcock, S. Draper, G.T. Houlsby, A.G.L. Borthwick and S. Serhadlıoğlu (2013) The available power from tidal stream turbines in the Pentland Firth, *Proc. R. Soc. Lond. A*, **469**(2157) 20130072.

[6] S. Draper, T. Stallard, P. Stansby, S. Way and T.A.A. Adcock (2013) Laboratory scale experiments and preliminary modeling to investigate basin scale tidal stream energy extraction, *10th European Wave and Tidal Energy Conference*, Aalborg, Denmark.

[7] M.B. Abbott and A.W. Minns (1979) *Computational Hydraulics*, Ashgate Publishing Co., Brookfield, Ct., Great Britain.

[8] P. García-Navarro, P. Brufau, J. Burguete, and J., Murillo (2008) The shallow water equations: an example of hyperbolic system, *Monografias de la Real Acadeia de Ciencias de Zaragoza*, vol. 31, pp. 89-119.

[9] G.E. Karniadakis and S. Sherwin (2005) *Spectral/hp element methods for computational fluid dynamics,* 2nd ed., New York: Oxford Science Publication.

[10] B. Cockburn and C.W. Shu (1998) The Runge-Kutta discontinuous Galerkin finite element method for conservation laws V: multidimensional systems, *Journal of Computational Physics*, **121**:2, pp. 199-224.

[11] B. Cockburn and C.W. Shu (2001) Runge-Kutta Discontinuous Galerkin methods for convection-dominated problems, *Journal of Scientific Computing*, **16**:3, pp. 173-266.

[12] E.J. Kubatko, J.J. Westerink and C. Dawson (2006) *hp* discontinuous Galerkin methods for advection dominated problems in shallow water flow, *Comput. Methods Appl. Mech. Engrg*., **196**, pp. 437-451.

[13] G.T. Houlsby, S. Draper, M.L.G. Oldfield (2008) Application of Linear Momentum Actuator Disc Theory to open channel flow, Technical report, Department of Engineering Science, University of Oxford, UK.

[14] S.Serhadlıoğlu, G.T. Houlsby, T.A.A. Adcock, S. Draper and A.G.L. Borthwick (2013) Assessment of tidal stream energy resources in the UK using a discontinuous Galerkin finite element scheme, *17th International Conference on Finite Elements in Flow Problems*, San Diego, California.

[15] M.J. Howarth, *Currents in the eastern Irish Sea*, Oceanography and Marine Biology, An Annual Review, **22**, pp. 2-47, Aberdeen University Press, 1984.

[16] S. Bunya, E.J. Kubatko, J.J. Westerink, and C.A. Dawson (2009) A wetting and drying treatment for the Runge-Kutta discontinuous Galerkin solution to the shallow water equations, *Compt. Methods Appl. Mech. Engineering*, **198**, pp.1548-1562.

[17] Admiralty Tide Tables Vol.1, United Kingdom and Ireland, Including European Channel Ports, 1997.

[18] D.T. Pugh (1987) *Tides, surges and mean sea-level*, John Wiley & Sons, Chichester.

[19] G. Godin (1983) On the predictability of currents, *International Hydrographic Review*, Monaco, LX (1).

[20] I.G. Bryden, S.J. Couch, A. Owen and G. Melville (2006) *Tidal current resource assessment*, *Proc. IMechE*, **221**, Part A: J. Power and Energy, pp. 125-135.

[21] P.K. Stansby (2006) Limitations of depth-averaged modelling for shallow wakes, *Journal of Hydraulic Engineering*, **132**, pp: 737-740.

[22] R. Vennell (2011) Tuning tidal turbines in-concert to maximize farm efficiency, *Journal of fluid mechanics,* **671**, pp. 587-604.

[23] T.A.A. Adcock and S. Draper (2014), Power extraction from tidal channels – multiple tidal constituents, compound tides and overtides, *Renewable Energy* (accepted).

[24] S. Draper, T.A.A. Adcock, G.T. Houlsby and A.G.L. Borthwick (2014) Estimate of the extractable Pentland Firth tidal stream power resource, *Renewable Energy* (accepted).

[25] S. Draper, T.A.A. Adcock, G.T. Houlsby and A.G.L. Borthwick (2014) An electrical analogy for the Pentland Firth tidal stream power resource, *Proceedings of Royal Society A* (accepted).